Chemical Research in Toxicology

ARTICLE

pubs.acs.org/crt

Cellular Responses Associated with Dibucaine-Induced Phospholipidosis

Ana Peropadre, Paloma Fernández Freire, Óscar Herrero,[†] José M. Pérez Martín, and M[a] José Hazen*

Cellular Toxicology Group, Laboratory A-110, C/Darwin 2, 28049 Madrid, Spain

Department of Biology, Faculty of Science, Universidad Autónoma de Madrid, Spain

ABSTRACT: A wide range of cationic amphiphilic drugs (CADs) from different therapeutic areas are known to cause phospholipidosis both *in vivo* and *in vitro*. Although the relevance of this storage disorder for human health remains uncertain, CADs have been repeatedly associated with clinical side effects, and as a result, phospholipidosis is of major concern for drug development in the pharmaceutical industry. An important unresolved question in this field is whether phospholipidosis is really linked to cellular toxicity. This work was focused on studying cellular responses associated with CAD-induced phospholipidosis in cultured mammalian kidney cells. Dibucaine (2-butoxy-*N*-[2-diethylaminoethyl]quinoline-4-carboxamide), an amide-type anesthetic with poorly defined cytotoxic effects, was used to induce phospholipidosis in Vero cells. The results from several assays that measure cell viability, proliferation, and morphological changes indicated that dibucaine-induced lysosomal phospholipidosis was accompanied by cellular defense responses such as transient growth arrest and autophagy, under mild stress conditions. Conversely, when tolerance limits were exceeded treated Vero cells underwent extensive and irreparable injury, leading ultimately to cell death. Our data provide additional information that may be of considerable interest for drug safety assessment.

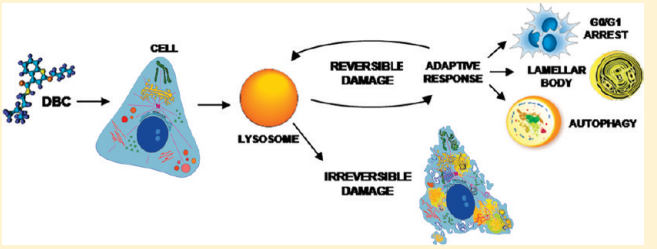

1. INTRODUCTION

Drug-induced phospholipidosis (PLD) is characterized by an excessive accumulation of phospholipids in lysosomes and by the appearance of membranous lamellar inclusions known as myeloid bodies.[1] A wide range of cationic amphiphilic drugs (CADs), including antidepressants, antiarrythmics, antibiotics, cholesterol-lowering agents, and local anesthetics, cause phospholipidosis in animals and humans.[2,3] The mechanisms responsible for PLD are complex, as shown in recent reviews on this subject[1,4−6] and may involve the formation of indigestible CAD-phospholipid complexes, direct inhibition of lysosomal phospholipases, and alterations in the biosynthesis and turnover of phospholipids. Moreover, it has also been reported that an increase in cellular cholesterol content is related to phospholipidosis induction.[7,8] Although the relevance of this storage disorder for human health remains uncertain, drugs that produce PLD are repeatedly associated with clinical side effects, such as liver, kidney, or respiratory failure.[3,5,9] Consequently, phospholipidosis has become nowadays a major concern in the course of drug development.[10−12] Despite the numerous high-throughput methods that have been proposed, a combination of in vivo, in silico, and in vitro cell-based approaches constitutes the most recent proposal for the prediction or screening of PLD.[13,14] However, an important limitation of research in this field is the scarcity of studies that assess the response of the cells to the presence of PLD.[4] Some attempts have been made to examine the hepatotoxicity of PLD-inducing drugs using gene expression arrays on rat liver[15] and human HepG2 cells,[16−18] since changes in mRNA (mRNA) expression appears to be one of the earliest events in cellular stress and/or tissue damage. Conversely, although PLD has been described in the human kidney,[19−23] very few studies have specifically examined whether excessive phospholipid accumulation might contribute to toxicity in cells of renal origin. This is of particular importance because nephrotoxicity that manifests during drug development or clinical practice can lead, in a significant number of cases, to acute kidney injury.[24]

The aim of this work was to provide a comprehensive description of the potential changes in essential cell functions and structures that could be associated with phospholipidosis. Since reliable cell-based models may contribute to PLD assessment, a cell line derived from African green monkey kidney (Vero) previously proved to be suitable for evaluating chemical-induced cytotoxicity as well as nephrotoxicity[25−28] was selected for the study. However, induction of phospholipidosis was achieved by treatment with dibucaine (2-butoxy-*N*-[2-diethylaminoethyl]quinoline-4-carboxamide), a potent amide anesthetic that interacts strongly with polar lipids causing lysosomal PLD.[29] Another reason that prompted us to choose this compound is that, although it has been reported that dibucaine (DBC) impairs mitochondrial function,[9,30−33] alters cell membrane properties,[34,35] and exhibits both apoptotic[36,37] and antiapoptotic activities,[38,39] the cytotoxicity of this cationic amphiphilic drug is

Received: August 2, 2010
Published: January 24, 2011

poorly characterized in non-neuronal cell models. This study was carried out using a number of mechanistically relevant end points that measure cell proliferation, viability, and morphological changes according to the guidelines of the Interagency Coordinating Committee on the Validation of Alternative Toxicological Methods.[40] Our results contribute to the understanding of cellular responses associated with CAD-induced phospholipidosis and supply additional information for drug safety assessment in preclinical trials.

2. EXPERIMENTAL PROCEDURES

2.1. Cell Culture and DBC Treatments. Vero cell line (ATCC number CCL-81) was routinely grown at 37 °C in a 5% CO_2 humidified atmosphere, using Dulbecco's modified Eagle's medium (DMEM), supplemented with 5% fetal calf serum, 100 IU/mL penicillin, 100 mg/mL streptomycin, and 2 mM L-glutamine (Lonza, Switzerland). Exponentially growing cells were seeded at a density of 10^5 cells/mL in different cell culture surfaces (Falcon, Becton Dickinson, USA), depending on the experimental procedure. After an overnight incubation, cells were exposed to concentrations of dibucaine (DBC) ranging from 1 to 100 μM (0.34−34 mg/mL). At given times during the experimental period, both treated and untreated cells were gently washed with phosphate-buffered saline (PBS) and processed according to the different experimental analyses.

Stock solutions of DBC (CAS number 85-79-0, Sigma, USA) were made in PBS and maintained in darkness at room temperature. The exposure solutions were prepared before use in DMEM with 1% serum and sterilized by filtration through a 0.22 μm Millipore filter.

2.2. Cytotoxicity Assays. Acute cytotoxicity was evaluated by four quantitative spectrophotometric methods on Vero cells grown in 24-well plates and treated with increasing concentrations of DBC during 24 h.

Cell number was estimated by quantifying total protein content (TPC) according to the method of Bradford in 1976,[41] using Coomassie Brilliant Blue G-250 reagent and bovine serum albumin as standard. MTT assay, that involves the reduction of the tetrazolium salt (3-[4,5-dimethylthiazol-2-yl]-2,5 diphenyltetrazolium bromide) by viable cells to purple formazan, was performed according to the method of Mossmann.[42] Neutral red uptake (NRU) into lysosomes of viable cells was evaluated as described by Borenfreund and Puerner.[43] The activity of intracellular LDH (EC1.1.1.27) as a measure of cell membrane integrity was determined with the UV method[44] by quantifying the decreasing amounts of NADH (Sigma) in the presence of sodium pyruvate as the substrate.

The absorbance values for the different cytotoxicity assays were recorded at appropriate wavelengths (TPC, 595 nm; MTT, 570 nm; NRU, 542 nm; LDH, 340 nm) using a Spectrafluor microplate reader (Tecan, Austria).

2.3. Cell Proliferation Assessment. To evaluate the effect of DBC in Vero cell proliferation and/or detachment, three independent assays were carried out. The determination of mitotic index was performed in cells growing on glass coverslips into 6-well culture plates. After 24 h exposure to DBC, cells were fixed with cold methanol and stained with 5 μg/mL Hoechst 33258 (Riedel de Haen, Germany). Three thousand cells were counted at each dose point, and the mitotic index (MI) was calculated as the ratio between the number of cells in mitosis and the total number of cells.

Likewise, cells were seeded in 25 cm^2 culture flasks and exposed to DBC concentrations during 24 h for flow cytometry analysis of DNA content. After the treatments, floating and adherent cells were collected (by trypsinization when needed) and centrifuged at 1500 rpm for 10 min. After a rinse in PBS and subsequent centrifugation, the pellet was fixed in 1 mL of 70% ice-cold ethanol during at least 18 h. Before measurement, cells were centrifuged and incubated for 30 min in a solution containing 50 μg/mL RNase A (Sigma) and 50 μg/mL propidium iodide (Sigma) in 0.1% sodium citrate buffer (Merck). Measurements were carried out in a Coulter Epics XL-MCL (Beckman Coulter, USA) cytometer equipped with an argon laser (488 nm) and the appropriate photomultiplier to recover 620 nm light. Data were analyzed with Expo 32 ADC software (Beckman Coulter).

Cell detachment after DBC treatments was determined in 25 cm^2 flasks by counting the number of floating and, after trypsinisation, adherent cells with a Bürker chamber (Marienfeld, Germany). In parallel, adherent cells were pooled with floating cells and collected by centrifugation at 1200 rpm for 10 min. Pellets were then fixed in 100 μL of cold methanol and kept in the dark at −20 °C until used. Nuclear morphology was analyzed by staining with 1 mg/mL Hoechst 33258 (Riedel de Haen), differentiating between normal and abnormal nuclei, in at least 2000 nuclei per sample.

2.4. Morphological Evaluation. In a first set of experiments, Vero cells grown on sterile glass coverslips and treated for 24 h with 5 and 50 μM DBC were observed under conventional phase-contrast and fluorescence microscopy to assess possible changes in critical subcellular structures including the cytoskeleton. For the evaluation of lysosomes and mitochondrial integrity, cells were incubated for 8 min in complete culture medium with 10 μM acridine orange (BDH, UK) or 17 μM rhodamine 123 (Sigma), respectively, and then observed under blue exciting light as a wet preparation.

To analyze the microtubule network, cells were fixed in methanol at −20 °C for 6 min and permeabilized with 0.5% (v/v) Triton X-100 in PBS for 5 min at room temperature. After blocking with 5% BSA (Sigma), cells were incubated with mouse monoclonal antibody (anti-α tubulin, Sigma) for 1 h at 37 °C, rinsed in PBS for 15 min, and subjected to fluorescein isothiocyanate (FITC)-labeled antimouse IgG (Sigma) for an additional 30 min at 37 °C. After nuclear counterstaining with 5 μg/mL Hoechst 33258 (Riedel de Haen) and a final rinse in PBS for 5 min, cells were mounted in ProLong Gold antifade reagent (Invitrogen, USA).

For the staining of microfilaments, cells were fixed in Formol-PBS (1:10) for 10 min and permeabilized with 0.5% (v/v) Triton X-100 in PBS for 5 min, at room temperature. Afterward, they were incubated with (TRITC)-labeled phalloidin (Sigma) for 20 min at 37 °C, washed in PBS, and mounted in ProLong (Invitrogen).

Microscopic observations were performed using an Olympus BX-61 epifluorescence microscope (Tokyo, Japan), equipped with an HBO 100 W mercury lamp and ultraviolet (UV, 365 nm), blue (450−490 nm), and green (546 nm) excitation filters. The images were acquired with a CCD camera Olympus DP-70 and processed using the software Olympus DP controller 1.1.1.65 and Adobe Photoshop 8.0. (Adobe Systems Inc., USA). All comparative images (treated vs untreated samples) were obtained under identical microscope and camera settings.

To confirm the ability of DBC to induce phospholipidosis and further investigate the intracellular targets of the compound, an ultrastructural analysis was conducted as previously described[45] using a JEOL JEM 1010 transmission electron microscope, operated at an accelerating voltage of 80 kV.

2.5. Reversibility of DBC Effects. To test whether the effect of DBC on the lysosomal compartment was reversible, Vero cells exposed to the compound during 4 and 24 h were incubated for an additional 24 h with fresh culture medium. Subsequently, cell cultures were reassayed for protein content and uptake of neutral red, as described previously.

2.6. Statistical Analysis. Experiments were performed at least three times and each concentration group was assayed using triplicated wells. Concentration−response cytotoxicity curves were generated with individual data points expressed as a percentage of that found in untreated cultures and presented as the arithmetic mean ± standard

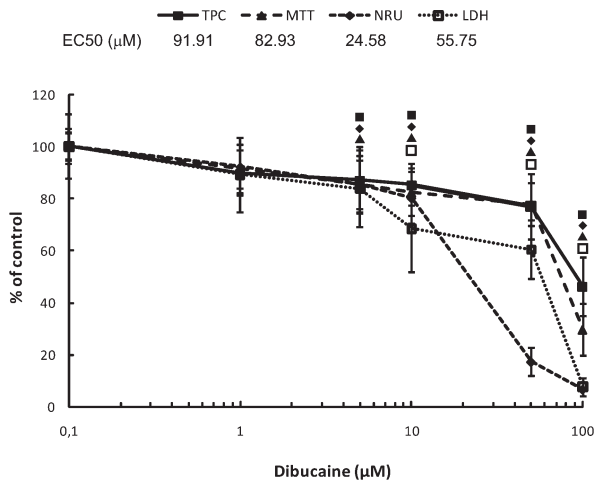

Figure 1. Dose−response curves obtained in the four cytotoxicity assays (■, TPC; ▲, MTT; ♦, NRU; □, LDH) after the treatment of Vero cells for 24 h with increasing DBC concentrations. The values represent the mean ± SD from three independent determinations, and the symbols indicate statistically different values in treated cells compared to those of control cells. The EC50 values for the different parameters are shown on top.

deviation using Microsoft Excel 2007. Statistical analysis, including analysis of variance (ANOVA) with the appropriate post hoc test (Bonferroni or Games-Howell) and nonlinear regression for the determination of the EC50 values, were carried out using GraphPad Prism 4.0 for windows (GraphPad Software Inc., USA). The level of statistical significance was in all cases $p \leq 0.05$.

3. RESULTS

3.1. Effects on Cell Viability and Proliferation Induced by DBC. Dose−response curves, obtained with the four assays employed to evaluate DBC-induced cytotoxicity in Vero cells, are depicted in Figure 1. The data reveal that exposure of Vero cells to DBC for 24 h, resulted in a dose-dependent cytotoxic effect that was statistically significant at concentrations ≥5 μM (TPC, MTT, NRU) or 10 μM (LDH). Membrane-based methods were the most sensitive, in particular the NRU assay, with EC50 values more than 2-fold lower than those estimated when the LDH leakage test was employed, which suggests specific injury in the endosomal/lysosomal compartment of Vero cells after DBC exposure.

Cell proliferation was also severely affected by DBC treatments, as indicated by a significant and dose-related decrease in mitotic indices, from the lowest concentration tested (5 μM), and the cessation of mitotic activity when Vero cells were exposed to the compound at a concentration of 100 μM (Table 1). Flow cytometric analysis of the cell cycle confirmed the antiproliferative effect of DBC and revealed a significant reduction in the S and G2/M fractions at concentrations ≥10 μM that was accompanied by an accumulation of cells in G0/G1 phase after treatments with 50 μM DBC (Figure 2).

Likewise, a significant and dose-dependent increase in the number of floating cells in the medium was observed in cell cultures incubated for 24 h with 50 and 100 μM DBC. In these same experimental conditions, fluorescence microscopy revealed pyknotic nuclei compatible with cell death in treated cultures (Figure 3).

3. 2. Morphological Changes in Vero Cells Exposed to DBC. As shown in Figure 4, phase contrast microscopy demonstrated that DBC produced severe cellular retraction and the appearance of dense granules in the cytoplasm, even at the lowest concentration tested (5 μM). No evident changes in the mitochondria were observed, except for a slight fragmentation in cells treated with DBC concentrations ≥50 μM. The endosomal compartment exhibited a dose-dependent alkalinization, shown as a shift in lysosomal fluorescence from red toward yellow or orange, accompanied by swelling after acridine orange (AO) staining. The evaluation of cytoskeletal components determined that the patterns of actin were disturbed, with a loss of stress fibers at low DBC concentration (5 μM) and the presence of severed microfilaments at the highest concentration studied (50 μM). On the contrary, the same DBC exposure conditions did not affect the appearance of the microtubule network in Vero cells.

A deeper insight into the subcellular alterations observed in treated Vero cells was acquired by TEM. Control cells showed a normal ultrastructure with uncondensed chromatin and well-preserved organelles (Figure 5A). Following treatments with 50 μM DBC, the most striking ultrastructural modification was an extensive vacuolization of the cytoplasm, suggesting the induction of autophagy (Figure 5B). When treated cultures were observed in detail, all the cells showed myeloid bodies, confirming phospholipidosis, as well as autophagosomes and autolysosomes (Figure 5 C-E). However, we found no occurrence of ultrastructural changes in cell organelles including mitochondria (Figure 5F). The features previously described were common to all the cells, although, occasionally, injury was more severe, and some cells exhibited a characteristic pattern of death (Figure 5G).

3. 3. Additional Studies on DBC-Induced Lysosomal Injury. Since the endosomal compartment was identified as the major intracellular target of DBC in Vero cells, further analyses were conducted to assess the extent and/or reversibility of cytotoxic effects. Despite an apparent recovery in NRU observed 4 h after drug removal, we selected a 24 h recovery time taking into consideration cell proliferation. Therefore, both total protein content and the uptake of NR were reassessed 24 h after drug removal in cells pretreated with DBC for 4 and 24 h. Taking into account that the 4 h NRU EC50 value (29.42 μM) was not significantly different from that previously obtained after a 24 h exposure (Student's *t* test, $p \leq 0.05$), this short exposure time was included in the reversibility assays.

As shown in Figure 6, dose−response curves for cell cultures pretreated with DBC concentrations up to 10 μM during 4 or 24 h were able to restore normal protein content levels during the recovery period. Conversely, treatments with 50 or 100 μM DBC for 4 or 24 h did not permit a complete recovery after 24 h and significant differences with the respective controls were detected. However, the parallel evaluation of NRU in these same conditions revealed higher amounts of incorporated dye than expected in view of TPC results, reaching values even higher than those of control untreated cells with concentrations up to 10 μM DBC.

4. DISCUSSION

Given the complexity of toxicity pathways and the functional interactions between the main components of animal cells, cytotoxicity results may differ depending on the end point utilized.[46] Consequently, different assays were performed to comprehensively evaluate the potential relationship between PLD and

Table 1. Mitotic Index Scoring after 24 h of Treatment of Vero Cells with Increasing Concentrations of DBC[a]

	mitotic index (% C)				
DBC (μM)	0	5	10	50	100
M ± SD	100.00 ± 13.35	78.03 ± 3.67*	57.55 ± 9.26*	43.12 ± 1.65*	0.00 ± 0.00*

[a] Asterisks indicate statistically significant differences between treated and control cells.

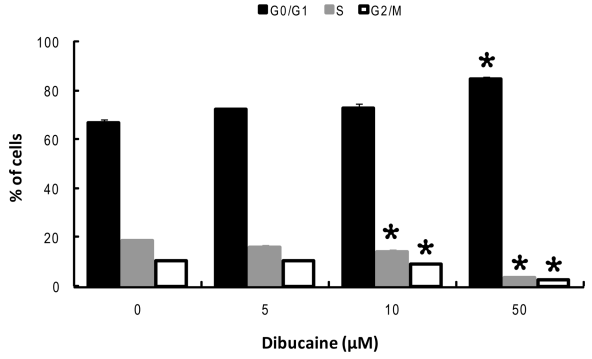

Figure 2. Cell cycle profiles of Vero cells exposed for 24 h to increasing concentrations of DBC. The values represent the mean ± SD of three independent experiments. Asterisks indicate statistically different values in treated cells compared to those in control cells.

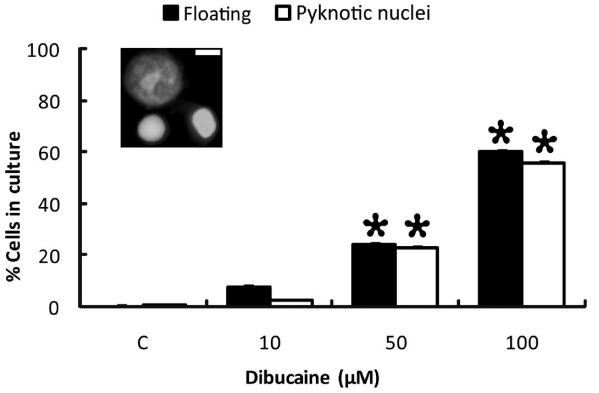

Figure 3. Percentage of floating cells and cells with pyknotic nuclei after exposure to different concentrations of DBC during 24 h. The values represent the mean ± SD from three independent experiments, and asterisks indicate statistically different values in treated cells compared to those in control cells. The image at the top left of the figure is a representative Hoechst fluorescence micrograph showing pyknotic and normal nuclei of Vero cells treated with 50 μM DBC. Bar = 5 μm.

cytotoxicity in mammalian kidney cells, as well as to ensure the accuracy and reliability of our data. Overall, results from this study demonstrated that lysosomal phospholipidosis induced by DBC in Vero cells was associated with considerable cytotoxic effects including the disruption of actin cytoskeleton, induction of autophagy, impairment of the proliferative activity, and triggering of cell death.

Lysosomal alkalinization represented an early alteration in DBC-treated cells that was hardly surprising, considering the physicochemical properties of the compound. Dibucaine is a lipophilic molecule[47] belonging to the CADs group that shares a common structure consisting of a hydrophobic ring system and a hydrophilic domain, with one or more primary or substituted nitrogen groups.[48] Both cationic and uncharged species of DBC coexist at physiological pH and interact with bilayer membranes,[49] whereas in acidic milieus, the compound is rapidly taken up and accumulates in its protonated form.[50] It is well known that a rise in lysosomal pH, as detected by AO staining in Vero cells, may indirectly alter the activity of some enzymes such as phospholipases or the supply of newly sinthesized enzymes toward the lysosomal compartment, resulting in phospholipidosis.[51] However, there is also evidence that DBC reduces sphingomyelinase activity in human fibroblasts,[52] inhibits phospholipase A2 (PLA2) in different membrane systems by interaction with the substrate,[53] and may alter phospholipid metabolism.[54] Therefore, the possibility that DBC could operate by different mechanisms, which are not necessarily mutually exclusive, cannot be ruled out. However, although drug lysosomotropism may result in intracellular storage of defective material, causing alterations in cell homeostasis and even cell death,[55] it may also considerably reduce the drug distribution, thus protecting critical targets against toxic injuries. This could explain the minimal mitochondrial damage observed in DBC-treated Vero cells, in contrast with that reported using isolated mitochondria.[31]

However, fluorescence microscopy analysis demonstrated that DBC causes a dose-dependent cellular retraction and disruption of the actin cytoskeleton but did not alter the microtubule network of Vero cells. It is well established that tertiary amine local anesthetics activate phospholipase C and consequently may interfere with membrane-associated cytoskeletal organization.[56] However, our results might also be related to the ability of DBC to activate calpains,[57,58] a family of nonlysosomal cysteine proteases implicated, among other processes, in actin cytoskeleton organization beneath the plasma membrane.[59,60] Interestingly, it has been reported that calpains mediate increases in plasma membrane permeability through the proteolysis of cytoskeletal proteins during acute renal cell injury.[61] In support of this assumption, we observed that the extent of actin filament disruption was related with progressive LDH release from Vero cells. It is also worth mentioning that calpains are required in mammalian cells for the formation and maturation of autophagosomes during autophagy.[62,63] Autophagy is a regulated pathway involving the sequestration of damaged biomolecules and organelles into double-membrane autophagosomes that fuse with lysosomes for degradation.[64,65] Mammalian cells undergo this catabolic process at a basal level for the turnover of cytoplasmic components, but autophagy also constitutes an adaptive mechanism activated in response to stress, that can promote cell survival or cell death.[66,67] Besides, it should be stressed that recent evidence suggests a potential role of autophagy in the modulation of cellular lipid metabolism.[68] In line with this hypothesis, it was shown that increased autophagy is triggered to remove intracellular accumulation of lipids, produced either experimentally[69,70] or as a consequence of lysosomal storage diseases.[71,72] Our results are in agreement with this emerging view and suggest that autophagy was induced in Vero cells, in an attempt to reduce phospholipidosis caused by DBC. In fact, following a recovery period of 24 h, cells exposed for 4 or

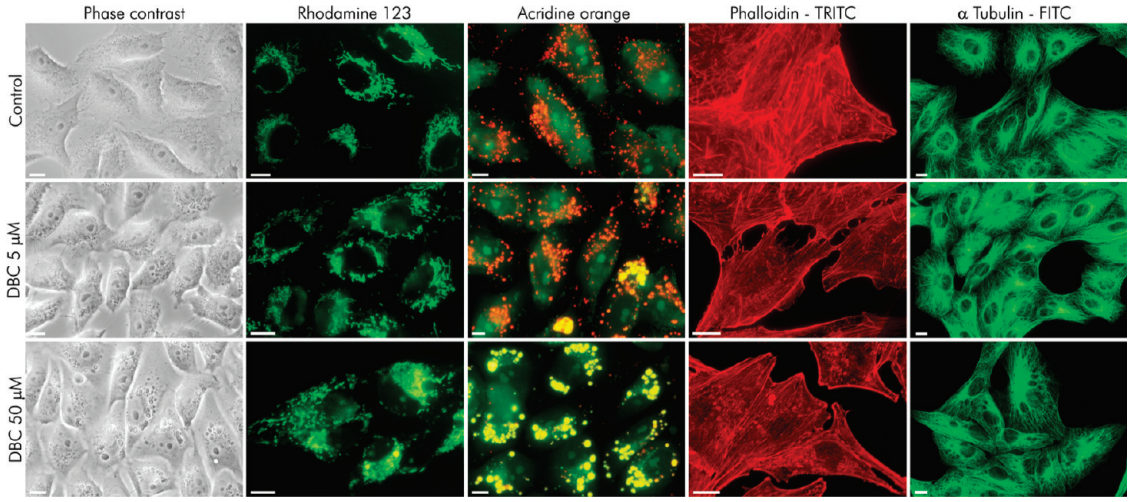

Figure 4. Microscopical analysis of Vero cells treated with different DBC concentrations for 24 h. Representative photomicrographs of the morphological appearance, mitochondrial reticulum, endosomal compartment, actin cytoskeleton, and microtubule network are shown from left to right. Bar = 10 μm.

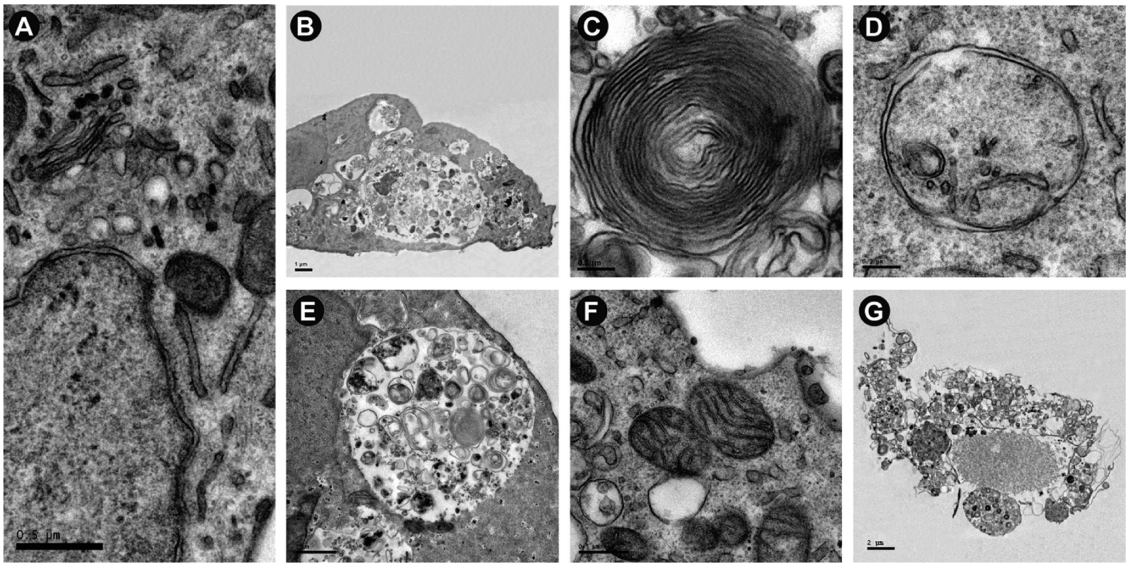

Figure 5. Representative images of Vero cells obtained by transmission electron microscopy. Perinuclear cytoplasm of an untreated control cell showing normal ultrastructure (A). Intense cytoplasmatic vacuolization after a 24 h exposure to 50 μM DBC (B). Closer examination of a lamellar body (C) and an autophagosome (D) in cells treated for 4 h. Autolysosome containing amorphous and multillamellar structures (E) and preserved mitochondria (F) following a 24 h incubation period with the drug. Vero cell treated for 24 h with DBC, showing extensive autophagy and irreparable injury (G).

24 h to drug concentrations $\leq$50 μM regained the ability to incorporate neutral red, even in higher amounts than those in respective control cells.

Another notable finding in our study was the dose-dependent antiproliferative activity exerted by DBC on Vero cells. To our knowledge, this is the first report showing that this local anesthetic causes cell cycle arrest in mammalian cells. Although not yet clearly defined, several studies have revealed a connection between autophagy and cell cycle regulation.[73,74] Furthermore and most remarkably, it has been suggested that cell proliferation may be secondarily inhibited as a result of the accumulation of intracellular phospholipids.[18] Consistent with this possibility, the recovery experiments indicated that Vero cells treated with DBC at low to intermediate doses (up to 10 μM) resumed proliferation, while cells exposed to higher concentrations were not able to restore normal proliferative levels during the observed period. In addition, it should be mentioned that a significant proportion of floating cells showing highly pyknotic nuclei was observed in the culture medium, after exposure to high concentrations of the compound. This nuclear staining pattern is indicative of cellular demise, but the determination of the death pathway triggered by DBC on Vero cells was beyond the scope of the current study and deserves additional investigation.

We then conclude that lysosomal PLD in mammalian kidney cells might be considered an adaptive cellular response that is closely associated with transient growth arrest and autophagy. However, above a certain threshold cell cultures failed to recover following treatments and reached the point of no return that ultimately results in cell death. Consequently, further studies are underway to gain a complete understanding of the significance of

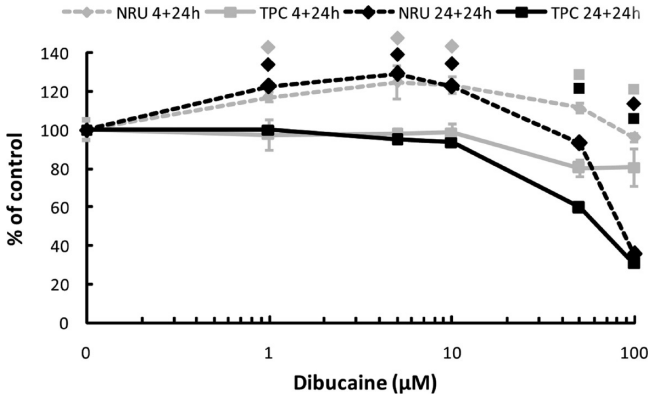

Figure 6. Assessment of TPC and NRU 24 h after drug removal in Vero cells pretreated with DBC for 4 and 24 h. Gray diamond, NRU 4 + 24 h; gray square, TPC 4 + 24 h; black diamond, NRU 24 + 24 h; black square, TPC 24 + 24 h. The symbols represent statistically significant differences between treated and respective control cultures.

chemical-induced phospholipidosis side effects in mammalian cultured cells. Finally, it is important to point out that dibucaine was earlier restricted to spinal anesthesia, due to its serious systemic effects on both the central nervous and cardiovascular system.[75] At present, even though it may cause allergic dermatitis,[76,77] DBC is just utilized for topical anesthesia as over-the-counter creams to relieve pain and itching caused by minor burns, insect bites, and hemorrhoids. Therefore, the failure of some organ function as a side effect of DBC use seems very unlikely.

AUTHOR INFORMATION

Corresponding Author

*Phone: +34 914978248. Fax: +34914978344. E-mail: mariajose.hazen@uam.es.

Present Addresses

[†]Grupo de Biología y Toxicología Ambiental, Departamento de Física Matemática y de Fluidos, Facultad de Ciencias-UNED, Paseo de la Senda del Rey 9, Madrid 28040, Spain.

Funding Sources

This work was supported by a grant (CTM2008-00311) from the Spanish Ministry of Science and Innovation. A.P. is a recipient of a contract from the Community of Madrid (Contrato de Personal Investigador de Apoyo).

ACKNOWLEDGMENT

We thank Sylvia Gutierrez Erlandsson for technical assistance.

ABBREVIATIONS

AO, acridine orange; CADs, cationic amphiphilic drugs; DBC, dibucaine; LDH, lactate dehydrogenase; NRU, neutral red uptake; TPC, total protein content; PLD, phospholipidosis.

REFERENCES

(1) Anderson, N., and Borlak, J. (2006) Drug-induced phospholipidosis. *FEBS Lett. 580*, 5533–5540.

(2) Halliwell, W. (1997) Cationic amphiphilic drug-induced phospholipidosis. *Toxicol. Pathol. 25*, 53–60.

(3) Reasor, M., and Kacew, S. (2001) Drug-induced phospholipidosis: are there functional consequences? *Exp. Biol. Med. 226*, 825–830.

(4) Alakoskela, J., Vitovi, P., and Kinnunen, P. (2009) Screening for the drug-phospholipid interaction: correlation to phospholipidosis. *ChemMedChem 4*, 1224–1251.

(5) Nonoyama, T., and Fukuda, R. (2008) Drug-induced phospholipidosis: pathological aspects and its prediction. *J. Toxicol. Pathol. 21*, 9–24.

(6) Reasor, M., Hastings, K., and Ulrich, R. (2006) Drug-induced phospholipidosis: issues and future directions. *Expert Opin. Drug Saf. 5*, 567–583.

(7) Hutchinson, T., Mahshid, Y., Jönsson, R., Björklund, C., and Kenne, K. (2008) Proteomic analysis of phospholipidosis in citalopram treated U937 cells: support for the cholesterol biosynthesis hypothesis. *Toxicol. in Vitro 22*, 1198–1204.

(8) Vejux, A., Malvitte, L., and Lizard, G. (2008) Side effects of oxysterols: cytotoxicity, oxidation, inflammation, and phospholipidosis. *Braz. J. Med. Biol. Res. 41*, 545–556.

(9) Tengstrand, E., Miwa, G., and Hsieh, F. (2010) Bis(monoacylglycerol)phosphate as a non-invasive biomarker to monitor the onset and time-course of phospholipidosis with drug-induced toxicities. *Expert Opin. Drug Metab. Toxicol. 6*, 555–570.

(10) Berridge, B. R., Chatman, L. A., Odin, M., Schultze, A. E., Losco, P. E., Meehan, J. T., Peters, T., and Vonderfecht, S. L. (2007) Phospholipidosis in nonclinical toxicity studies. *Toxicol. Pathol. 35*, 325.

(11) Ratcliffe, A. (2009) Medicinal chemistry strategies to minimize phospholipidosis. *Curr. Med. Chem. 16*, 2816–2823.

(12) Tengstrand, E., Lee, J., Alden, C., and Hsieh, F. (2007) Biomarkers to monitor drug-induced phospholipidosis. *Toxicol. Appl. Pharmacol. 218*, 72–78.

(13) Chatman, L. A., Morton, D., Johnson, T. O., and Anway, S. D. (2009) A strategy for risk management of drug-induced phospholipidosis. *Toxicol. Pathol. 37*, 997–1005.

(14) Hanumegowda, U., Wenke, G., Regueiro-Ren, A., Yordanova, R., Corradi, J., and Adams, S. (2010) Phospholipidosis as a function of basicity, lipophilicity, and volume of distribution of compounds. *Chem. Res. Toxicol. 23*, 749–755.

(15) Ennulat, D., Magid-Slav, M., Rehm, S., and Tatsuoka, K. (2010) Diagnostic performance of traditional hepatobiliary biomarkers of drug-induced liver injury in the rat. *Toxicol. Sci. 116*, 397–412.

(16) Atienzar, F., Gerets, H., Dufrane, S., Tilmant, K., Cornet, M., Dhalluin, S., Ruty, B., Rose, G., and Canning, M. (2007) Determination of phospholipidosis potential based on gene expression analysis in HepG2 cells. *Toxicol. Sci. 96*, 101–114.

(17) Nioi, P., Perry, B. K., Wang, E.-J., Gu, Y.-Z., and Snyder, R. D. (2007) *In vitro* detection of drug-induced phospholipidosis using gene expression and fluorescent phospholipid based methodologies. *Toxicol. Sci. 99*, 162–173.

(18) Sawada, H., Takami, K., and Asahi, S. (2005) A toxicogenomic approach to drug-induced phospholipidosis: analysis of its induction mechanism and establishment of a novel *in vitro* screening system. *Toxicol. Sci. 83*, 282–292.

(19) Albay, D., Adler, S., Phiposse, J., Calescibetta, C., Romansky, S., and Cohen, A. (2005) Chloroquine-induced lipidosis mimicking Fabry disease. *Mod. Pathol. 18*, 733–738.

(20) Bracamonte, E., Kowalewska, J., Starr, J., Gitomer, J., and Alpers, C. (2006) Iatrogenic phospholipidosis mimicking Fabry disease. *Am. J. Kidney Dis. 48*, 844–850.

(21) Loh, A., and Cohen, A. (2009) Drug-induced kidney disease: pathology and current concepts. *Ann. Acad. Med. Singapore 38*, 240–250.

(22) Muller-Hocker, J., Schmid, H., Weiss, M., Dendorfer, U., and Braun, G. (2003) Chloroquine-induced phospholipidosis of the kidney mimicking Fabry's disease: case report and review of the literature. *Hum. Pathol. 34*, 285–289.

(23) Pintavorn, P., and Cook, W. (2008) Progressive renal insufficiency associated with amiodarone-induced phospholipidosis. *Kidney Int. 74*, 1354–1357.

(24) Bonventre, J., Vaidya, V., Schmouder, R., Feig, P., and Dieterle, F. (2010) Next-generation biomarkers for detecting kidney toxicity. *Nat. Biotechnol. 28*, 436–440.

(25) Grosse, Y., Baudrimont, I., Castegnaro, M., Betbeder, A., Creppy, E. E., Dirheimer, G., and Pfohl-Leszkowicz, A. (1995) Formation of ochratoxin A metabolites and DNA-adducts in monkey kidney cells. *Chem.-Biol. Interact. 95*, 175–187.

(26) Golli-Bennour, E., Kouidhi, A., Abid-Essefi, S., Hassen, W., and Bacha, H. (2010) Cytotoxicity and genotoxicity induced by aflatoxin B1, ochratoxin A, and their combination in cultured Vero cells. *J. Biochem. Mol. Toxicol. 24*, 42–50.

(27) Pari, L., Murugavel, P., Sitasawad, S., and Kumar, K. (2007) Cytoprotective and antioxidant role of diallyl tetrasulfide on cadmium induced renal injury: an in vivo and in vitro study. *Life Sci. 80*, 650–658.

(28) Prashanth, K., Shashidhara, S., Kumar, M., and Sridhara, B. (2001) Cytoprotective role of *Solanum nigrum* against gentamicin-induced kidney cell (Vero cells) damage in vitro. *Fitoterapia 72*, 481–486.

(29) Jägel, M., and Lüllmann-Rauch, R. (1984) Lipidosis-like alterations in cultured macrophages exposed to local anaesthetics. *Arch. Toxicol. 55*, 229–232.

(30) Adade, A. B., Chignell, D., and Vanderkooi, G. (1984) Local anesthetics: a new class of partial inhibitors of mitochondrial ATPase *J. Bioenerg. Biomembr. 16*, 353–363.

(31) Chazotte, B., and Vanderkooi, G. (1981) Multiple sites of inhibition of mitochondrial electron transport by local anesthetics. *Biochim. Biophys. Acta 636*, 153–161.

(32) Dabadie, P., Bendriss, P., Erny, P., and Mazat, J. P. (1987) Uncoupling effects of local anesthetics on rat liver mitochondria. *FEBS Lett. 226*, 77–82.

(33) Stringer, B. K., and Harmon, H. J. (1990) Inhibition of cytochrome oxidase by dibucaine. *Biochem. Pharmacol. 40*, 1077–1081.

(34) Lee, Y., Park, N. S., Kwon, J. D., Park, J. S., Shin, G. B., Lee, C. S., Jung, T. S., Choi, N. J., Yoon, J. H., Ok, J. S., Yoon, U. C., Bae, M. K., Jang, H. O., and Yun, I. (2007) Amphiphilic effects of dibucaine·HCl on rotational mobility of n-(9-anthroyloxy)stearic acid in neuronal and model membranes. *Chem. Phys. Lipids 146*, 33–42.

(35) Malheiros, S. V. P., Brito, M. A., Brites, D., and Meirelles, N. C. (2000) Membrane effects of trifluoperazine, dibucaine and praziquantel on human erythrocytes. *Chem.-Biol. Interact. 126*, 79–95.

(36) Arita, K., Utsumi, T., Kato, A., Kanno, T., Kobuchi, H., Inoue, B., Akiyama, J., and Utsumi, K. (2000) Mechanism of dibucaine-induced apoptosis in promyelocytic leukemia cells (HL-60). *Biochem. Pharmacol. 60*, 905–915.

(37) Kim, M., Lee, Y. S., Mathews, H. L., and Wurster, R. D. (1997) Induction of apoptotic cell death in a neuroblastoma cell line by dibucaine. *Exp. Cell Res. 231*, 235–241.

(38) Martinez-Caballero, S., Dejean, L. M., and Kinnally, K. W. (2004) Some amphiphilic cations block the mitochondrial apoptosis-induced channel, MAC. *FEBS Lett. 568*, 35–38.

(39) Polster, B. M., Basanez, G., Young, M., Suzuki, M., and Fiskum, G. (2003) Inhibition of Bax-induced Cytochrome c release from neural cell and brain mitochondria by dibucaine and propranolol. *J. Neurosci. 23*, 2735–2743.

(40) ICCVAM. (2003) Guidelines for the Nomination and Submission of New, Revised, and Alternative Test Methods, National Institute for Environmental Health Sciences, Research Triangle Park, NC.

(41) Bradford, M. (1976) A rapid and sensitive method for the quantitation of microgram quantities of protein utilizing the principle of protein-dye binding. *Anal. Biochem. 72*, 248–254.

(42) Mosmann, T. (1983) Rapid colorimetric assay for cellular growth and survival: application to proliferation and cytotoxicity assays. *J. Immunol. Methods 65*, 55–63.

(43) Borenfreund, E., and Puerner, J. (1985) Toxicity determined *in vitro* by morphological alterations and neutral red absorption. *Toxicol. Lett. 24*, 119–124.

(44) Vassault, A. (1983) Lactate Dehydrogenase: UV Method with Pyruvate and NADH, in *Methods of Enzymatic Analysis* (Bergmeyer, H., Bergmeyer, J., and Grabl, M., Eds.) pp 118−126, Verlag Chemie, Weinheim, Germany.

(45) Pérez Martín, J., Labrador, V., Fernández Freire, P., Molero, M., and Hazen, M. (2004) Ultrastructural changes induced in HeLa cells after phototoxic treatment with harmine. *J. Appl. Toxicol. 24*, 197–201.

(46) Fellows, M. D., and O'Donovan, M. R. (2007) Cytotoxicity in cultured mammalian cells is a function of the method used to estimate it. *Mutagenesis 22*, 275–280.

(47) Lorite, G. S., Nobre, T. M., Zaniquelli, M. E. D., de Paula, E., and Cotta, M. A. (2009) Dibucaine effects on structural and elastic properties of lipid bilayers. *Biophys. Chem. 139*, 75–83.

(48) Reasor, M. (1997) Cation Amphiphilic Drugs, in *Comprehensive Toxicology, Vol. 8, Toxicology of the Respiratory System* (Sipes, I., McQueen, C., and Gandolfi, A., Eds.) pp 555−566, Elsevier Science, New York.

(49) Yun, I., Cho, E.-S., Jang, H.-O., Kim, U.-K., Choi, C.-H., Chung, I.-K., Kim, I.-S., and Wood, W. G. (2002) Amphiphilic effects of local anesthetics on rotational mobility in neuronal and model membranes. *Biochim. Biophys. Acta 1564*, 123–132.

(50) Schwarz, G., Damian, L., and Winterhalter, M. (2007) Model-free analysis of binding at lipid membranes employing micro-calorimetric measurements. *Eur. Biophys. J. 36*, 571–579.

(51) de Duve, C., de Barsy, T., Poole, B., Trouet, A., Tulkens, P., and Van Hoof, F. (1974) Lysosomotropic agents. *Biochem. Pharmacol. 23*, 2495–2531.

(52) Yoshida, Y., Arimoto, K., Sato, M., Sakuragawa, N., Arima, M., and Satoyoshi, E. (1985) Reduction of acid sphingomyelinase activity in human fibroblasts induced by AY-9944 and other cationic amphiphilic drugs. *J. Biochem. 98*, 1669–1679.

(53) Hendrickson, H. S., and van Dam-Mieras, M. C. (1976) Local anesthetic inhibition of pancreatic phospholipase A2 action on lecithin monolayers. *J. Lipid Res. 17*, 399–405.

(54) Allan, D., and Michell, R. (1975) Enhanced synthesis de novo of phosphstidylinositol in lymphocytes treated with cationic amphiphilic drugs. *Biochem. J. 148*, 471–478.

(55) Boya, P., and Kroemer, G. (2008) Lysosomal membrane permeabilization in cell death. *Oncogene 27*, 6434–6451.

(56) Raucher, D., and Sheetz, M. (2001) Phospholipase C activation by anesthetics decreases membrane-cytoskeleton adhesion. *J. Cell Sci. 114*, 3759–3766.

(57) Fox, J. (1999) On the role of calpain and Rho proteins in regulating integrin-induced signaling. *Thromb. Haemostasis 82*, 385–391.

(58) Oda, A., Druker, B., Ariyoshi, H., Smith, M., and Salzman, E. (1993) pp60src is an endogenous substrate for calpain in human blood platelets. *J. Biol. Chem. 268*, 12603–12608.

(59) Croall, D., and Ersfeld, K. (2007) The calpains: modular designs and functional diversity. *Genome Biol. 8*, 218.

(60) Suzuki, K., Hata, S., Kawabata, Y., and Sorimachi, H. (2004) Structure, activation, and biology of calpain. *Diabetes 53*, 12–18.

(61) Liu, X., and Schnellmann, R. (2003) Calpain mediates progressive plasma membrane permeability and proteolysis of cytoskeleton-associated paxillin, talin, and vinculin during renal cell death. *J. Pharmacol. Exp. Ther. 304*, 63–70.

(62) Demarchi, F., Bertoli, C., Copetti, T., Tanida, I., Brancolini, C., Eskelinen, E., and Schneider, C. (2006) Calpain is required for macroautophagy in mammalian cells. *J. Cell Biol. 175*, 595–605.

(63) Demarchi, F., and Schneider, C. (2007) The calpain system as a modulator of stress/damage response. *Cell Cycle 6*, 136–138.

(64) Ferraro, E., and Cecconi, F. (2007) Autophagic and apoptotic response to stress signals in mammalian cells. *Arch. Biochem. Biophys. 462*, 210–219.

(65) Xie, Z., and Klionsky, D. J. (2007) Autophagosome formation: core machinery and adaptations. *Nat. Cell Biol. 9*, 1102–1109.

(66) He, C., and Klionsky, D. J. (2009) Regulation mechanisms and signaling pathways of autophagy. *Annu. Rev. Genet. 43*, 67–93.

(67) Ravikumar, B., Futter, M., Jahreiss, L., Korolchuk, V. I., Lichtenberg, M., Luo, S., Massey, D. C. O., Menzies, F. M., Narayanan, U., Renna, M., Jimenez-Sanchez, M., Sarkar, S., Underwood, B., Winslow, A., and Rubinsztein, D. C. (2009) Mammalian macroautophagy at a glance. *J. Cell Sci. 122*, 1707–1711.

(68) Kovsan, J., Bashan, N., Greenberg, A. S., and Rudich, A. (2010) Potential role of autophagy in modulation of lipid metabolism. *Am. J. Physiol. Endocrinol. Metab. 298*, E1–7.

(69) Morissette, G., Ammoury, A., Rusu, D., Marguery, M. C., Lodge, R., Poubelle, P. E., and Marceau, F. (2009) Intracellular sequestration of amiodarone: role of vacuolar ATPase and macroautophagic transition of the resulting vacuolar cytopathology. *Br. J. Pharmacol. 157*, 1531–1540.

(70) Schmitz, G., and Grandl, M. (2009) Endolysosomal phospholipidosis and cytosolic lipid droplet storage and release in macrophages. *Biochim. Biophys. Acta 1791*, 524–539.

(71) Raben, N., Shea, L., Hill, V., Plotz, P., and Daniel, J. K. (2009) Monitoring Autophagy in Lysosomal Storage Disorders, in *Methods in Enzymology*, pp 417−449, Academic Press, New York.

(72) Settembre, C., Fraldi, A., Rubinsztein, D. C., and Ballabio, A. (2008) Lysosomal storage diseases as disorders of autophagy. *Autophagy 4*, 113–114.

(73) Gosselin, K., Deruy, E., Martien, S., Vercamer, C., Bouali, F., Dujardin, T., Slomianny, C., Houel-Renault, L., Chelli, F., De Launoit, Y., and Abbadie, C. (2009) Senescent keratinocytes die by autophagic programmed cell death. *Am. J. Pathol. 174*, 423–435.

(74) Lambert, L. A., Qiao, N., Hunt, K. K., Lambert, D. H., Mills, G. B., Meijer, L., and Keyomarsi, K. (2008) Autophagy: a novel mechanism of synergistic cytotoxicity between doxorubicin and roscovitine in a sarcoma model. *Cancer Res. 68*, 7966–7974.

(75) Heavner, J. E. (2008) Pharmacology of Local Anesthetics, in *Anesthesiology* (Longnecker, D., Ed.) pp 954−973, McGraw Hill Professional, New York.

(76) Hayashi, K., Kawachi, S., and Saida, T. (2001) Allergic contact dermatitis due to both chlorpheniramine maleate and dibucaine hydrochloride in an over-the-counter medicament. *Contact Dermatitis 44*, 56–57.

(77) Yoshika, Y., Naoki, O., Ayaka, H., Shigeru, K., and Akira, K. (2009) Allergic contact dermatitis from dibucaine hydrochloride, chlorpheniramine maleate, and naphazoline hydrochloride in an over-the-counter topical antiseptic. *Contact Dermatitis 61*, 52–53.